A&A 368, 580–592 (2001)
DOI: 10.1051/0004-6361:20010020

Astronomy & Astrophysics

Multimode δ Scuti stars in the open cluster NGC 7062⋆

L. M. Freyhammer[1,2], T. Arentoft[2], and C. Sterken[2,⋆⋆]

[1] Royal Observatory of Belgium, Ringlaan 3, 1180 Brussels, Belgium
[2] University of Brussels (VUB), Pleinlaan 2, 1050 Brussels, Belgium

Received 20 October 2000 / Accepted 21 December 2000

Abstract. The central field of NGC 7062 was observed intensively with the main goal of finding δ Scuti stars suitable for use in asteroseismological tests of stellar structure and evolution theory. BV time series photometry was obtained for this northern open cluster, which has a large population of stars inside the δ Scuti instability strip, making it a probable host of several such variables. We report findings of 15 pulsating stars, including at least 13 δ Scuti stars. Ten variables oscillate in two or more frequencies. Only one of these variables was known before, for which we detected 9 frequencies. Five probable variables are mentioned, and period analysis is given for all 20 stars.

Key words. stars: δ Scuti; evolution; oscillations – (galaxy:) open clusters and associations: individual: NGC 7062

1. Introduction

Multi–periodic δ Scuti stars are the most promising stars for comparative asteroseismological tests of stellar structure and evolutionary models. They oscillate in radial and non–radial modes and have conveniently short pulsation periods of a few hours and low, but measurable amplitudes of the order of a few mmag. They are main–sequence A–F stars, having masses of 1.5–2.5 $M_{\odot}$. The main difficulties in the application of asteroseismology to these variables are, from an observational point of view, to identify the pulsation modes, and to collect enough data to resolve the often very complex pulsational spectra of δ Scuti stars – and for detecting modes with sub–mmag amplitudes. Two main approaches are: (i) to concentrate on single stars and try to understand their pulsational behavior thoroughly, e.g. FG Vir (Breger et al. 1998), XX Pyx (Handler et al. 2000) and 4 CVn (Breger et al. 1999), or (ii) to study stellar clusters with populations rich in variables where constraints can be placed on the stellar models by assuming the same values for distance, age and metallicity.

A suitable open cluster for studying δ Scuti stars has an age of 0.3–1.0 Gyr and a distance of 1–2 kpc. Such a cluster has a convenient angular size in the sky and any population of δ Scuti stars will be among its brightest members (Frandsen & Arentoft 1998a). When good targets are found, worldwide multisite campaigns, organised by networks such as WET (Winget et al. 1993) and STACC (Frandsen et al. 2000) are needed to improve the spectral window, and rotational velocities and chemical compositions from multi–band photometry and spectroscopy are also required before asteroseismology can be attempted. Several interesting clusters are known in the southern sky, e.g. NGC 6134 (Frandsen et al. 1996), but few are known in the northern sky, under which the bulk of accessible small telescopes is located. Praesepe (Belmonte et al. 1994; Arentoft et al. 1998) with 18 δ Scuti stars, and NGC 1817 (Frandsen & Arentoft 1998b) with 8 δ Scuti candidates are examples of such clusters, however Praesepe's angular size of several degrees gives disadvantages. It is therefore important to find suitable northern clusters.

From the cluster target list by Frandsen & Arentoft (1998a,b) we selected NGC 7062, which is a well–studied cluster (e.g. Hoag et al. 1961; Peniche et al. 1990) but precise BV photometry is lacking. The photographic photometry from Hassan (1973) is the most recent, but has mean errors of $\pm 0\overset{\mathrm{m}}{.}03$ and $0\overset{\mathrm{m}}{.}04$ for V and $B-V$ respectively. Peniche et al. (1990) reported findings of 3 δ Scuti candidates in a field of the cluster, based on 14–15 measurements obtained in 3.5 contiguous hours. They found

Send offprint requests to: L. M. Freyhammer,
e-mail: lfreyham@vub.ac.be

⋆ Based on observations obtained at the Nordic Optical Telescope, operated on the island of La Palma jointly by Denmark, Finland, Iceland, Norway, and Sweden, in the Spanish Observatorio del Roque de los Muchachos of the Instituto de Astrofisíca de Canarias.

⋆⋆ Belgian Fund for Scientific Research (FWO).

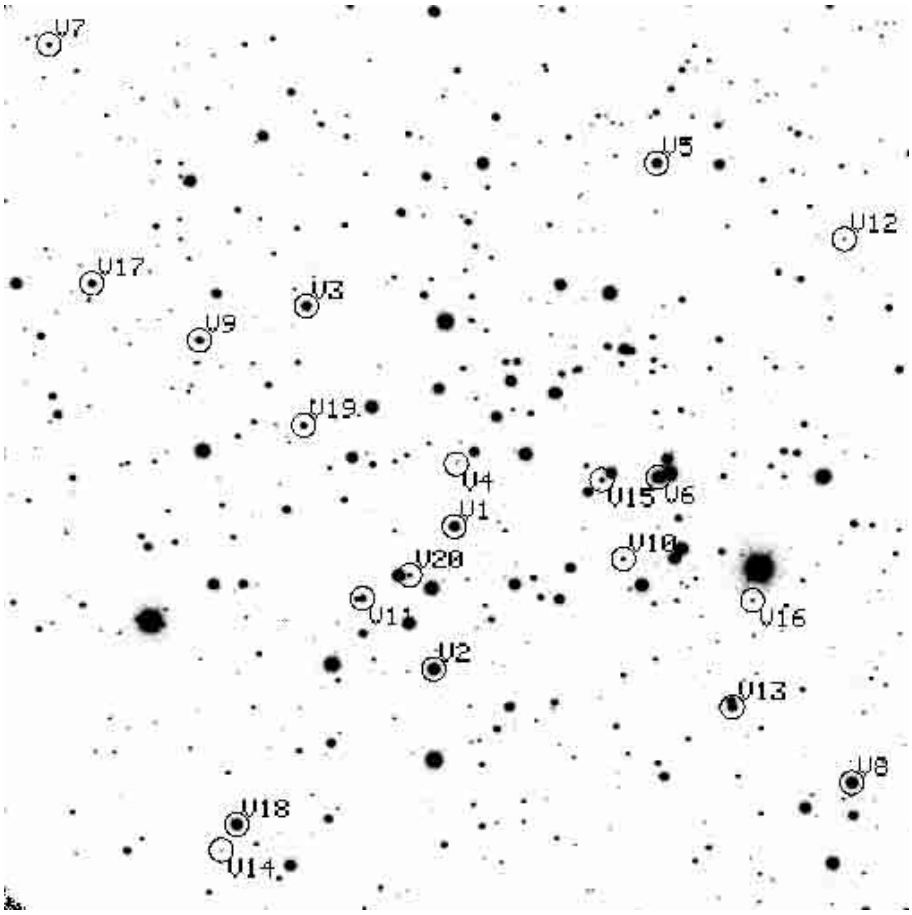

Fig. 1. 6′.5 by 6′.5 CCD frame of NGC 7062 with stars from Tables 2 and 3 indicated. N is up and E is right

abnormally high standard deviations of 2–3% in V for their ID 80, ID 13 and ID 17, which they considered as cluster members positioned in the δ Scuti region of the colour–magnitude diagram. Viskum et al. (1997) obtained 55 images of NGC 7062 and determined an age of 500 Myr and a distance of 1.8 ± 0.4 kpc. They also had the δ Scuti candidates ID 13 and ID 17 in their field but, although having only a few observations due to bad weather, they found that both stars are constant to 4 mmag. Instead these authors found a new, good, δ Scuti candidate – their #180.

For four nights on a medium–sized telescope, we have searched for δ Scuti stars among the members of NGC 7062. Only the observations and period analysis are presented here, since the baseline of the observations is too small to attempt mode identification.

2. Observations

The observations were collected with the 2.56 m Nordic Optical Telescope, La Palma, Canary Islands. The ALFOSC instrument was used with CCD#7 (2k × 2k LESSE-LORAL CCD having FOV = 6′.5, Fig. 1), read out in gain mode "HIGH" and single amplifier mode ("B"). The chip was uniform with only few large blemishes and had a readout noise of 5.5 e^- at a gain of 1.05 e^-/ADU.

Table 1. Log of the observations

Date UT	Length hours	Filter	No. of data pts	Exp. time s
19/08/00	8.5	B	164	50
		V	56	25
20/08/00	9.5	B	191	45
		V	64	20
21/08/00	5.0	B	74	40
		V	26	20
22/08/00	3.0	B	56	60
		V	19	30

Four nights were used for observing the cluster, as listed in Table 1. The first two nights had good and stable weather conditions, while the last half of the run was degraded by bad weather. A total of 26 hours of observation was obtained as series of 3× Bessel B, 1× Bessel V sequences. Typical light curves have 485 (B) and 160 (V) points, since only very few data points had to be rejected. The same field was observed during the whole run, centered on $\alpha_{2000.0} = 21^{\rm h}23^{\rm m}29^{\rm s}$ and $\delta_{2000.0} = 46°23'13''$. Exposure times were in optimal conditions 50 s in B and 25 s in V – but up to 5 min in bad weather. Dust was significant in the air the first two nights which increased exposure times at large air mass. Seeing conditions were

very stable and good – typically 1.″1. Pointing offsets for all nights were kept minimal – less than 2″. Exposure times were optimised for the $12^{\rm m}$ stars in the field so they could be used as good comparison stars.

3. Photometric reductions

During the first evening, a linearity test was performed using a β–light source to illuminate the detector. We found that up to 62 000 ADU per pixel, the deviation from linearity was less than 0.1 percent, giving a large dynamic range which was fully utilised in the observations. The images were properly bias–subtracted and flatfielded with sky flats using IRAF image reduction software. Some effects from light leaks in the instrument introduced differences between dusk and dawn flatfield images, but were averaged out by using multiple flatfields. Bad columns and cosmetic features on the CCD were smoothed by linear interpolation between neighbouring pixels using the IRAF task `proto.fixpix`.

Photometry was performed with the MOMF (Multi–Object–Multi–Frame) code appropriate for photometry in semi–crowded fields. MOMF performs a combined Point–Spread Function/Aperture (PSF/Ap) photometry for deriving stellar magnitudes, which gives high robustness over variations during the night, such as seeing changes or instrumental drift. Differential photometry was calculated with respect to a mean light level in each frame, giving stars with small scatter in the time series the highest weight in the calculation. MOMF is described in detail by Kjeldsen & Frandsen (1992). Photometric reductions were performed as described by Arentoft & Sterken (2000), using a PSF calculated on the basis of 10 stars carefully selected among 422 stars detected in a selected reference image. The PSF photometry is corrected by using Ap photometry in the cleaned image with 7 different apertures scaled with the seeing. The optimal aperture sizes were after preliminary reductions, found to be $1.2{-}3.0 \times FWHM$ (Full–Width–Half–Maximum) radius which were then fixed for all time series. $FWHM$ in the images was in general close to the recommended value of MOMF: 3–7 pixels. The local sky background was determined in an 8 pixel wide annulus outside the aperture of each star.

The best of our final light curves had intrinsic rms scatter of 1 mmag, but typically the scatter was 2–3 mmag. As will be discussed below, the rms scatter in the light curves are of the order of the theoretical values for shot noise and scintillation. Time series photometry was obtained for a sample of 422 stars present in all frames and spanning 8 magnitudes in brightness. The B–frames were reduced on a nightly basis, correcting for night–to–night offsets in the magnitude zero–points. This lowers the noise in the amplitude spectra, but alters the power at low frequencies (a few cycles per day, $\mathrm{c\,d^{-1}}$) reducing the reliability of significant frequencies. See e.g. Breger et al. (1993) for a discussion of this point. This correction was not applied to the less well–sampled V light curves.

To remove effects from extinction variation (e.g. due to the aforementioned dust in the atmosphere), cosmetic features and bad columns, we decorrelated each individual light curve by fitting the relative magnitudes to a function of the form:

$$V = a_0 + a_1 z + a_2 x + a_3 y + a_4 m + a_5 s, \quad (1)$$

where z is air mass, x, y are the x–, y–positions on the CCD relative to those on a fiducial frame, m is the level of local sky background and s is the $FWHM$ of the stellar profile. Coefficients significantly different from zero were typically a_1, in particular for red stars, a_2 when the stars were close to CCD blemishes and a_5 for stars with close neighbours. In practice the coefficients a_3 and a_4 were always close to zero. Decorrelation was applied to time strings with data from all nights and the effect of decorrelation was a decrease of noise in the amplitude spectra at low frequencies and had only minor effects on the strengths of peaks attributed to stellar oscillations. Figures 2a–d, illustrate this effect for a constant star, ID 143 ($V = 12\overset{\rm m}{.}9$, $B - V = 0\overset{\rm m}{.}5$). The raw light curve in Fig. 2c has a slow variation of 1–2 mmag amplitude which correlates with airmass. After decorrelation, this variation was removed from the light curve (Fig. 2d). In the two amplitude spectra, Figs. 2a and 2b, we see how the decorrelation efficiently removes a 2–3 $\mathrm{c\,d^{-1}}$ frequency and $1/f$ noise. A time string which is being decorrelated has to be significantly longer than the period of the star itself (Frandsen et al. 1996), so in a single case of a star with long periods ($V2$, see below) were the data were not decorrelated.

Because of the bad weather conditions in the last half of the run, we failed to observe standard stars. For this reason we tried instead to use the photographic UBV–photometry by Hassan (1973) to transform our data to the standard system. The transformation gave large transformation errors, perhaps due to misidentifications in their paper, and was thus rejected. Instead, we used their source for standard stars: Hoag et al. (1961), who published photoelectric and photographic measurements with mean errors for V: $\pm 0\overset{\rm m}{.}027$ and for $B - V$: $\pm 0\overset{\rm m}{.}033$. Four stars in common with our data had photoelectric measurements and 13 stars had photographic measurements. We used 12 of these to determine the transformation, using transformations of the types $B = B_i + a_0 + a_1(B - V)$ and $V = V_i + b_0 + b_1(B - V)$ where B_i and V_i are instrumental magnitudes. The accuracies of the transformations are for V: $\pm 0\overset{\rm m}{.}025$ and for $B - V$: $\pm 0\overset{\rm m}{.}040$.

3.1. Photometric quality

The theoretical noise in the light curves is, even for the brightest stars, dominated by photon shot noise. Contributions from shot noise and scintillation have been calculated using the Eqs. (3)–(4) from Kjeldsen & Frandsen (1992), and the shot noise is given in Col. 12 of Tables 2–3. The filter equivalent width, including all transmissions through telescope and instrument, was measured

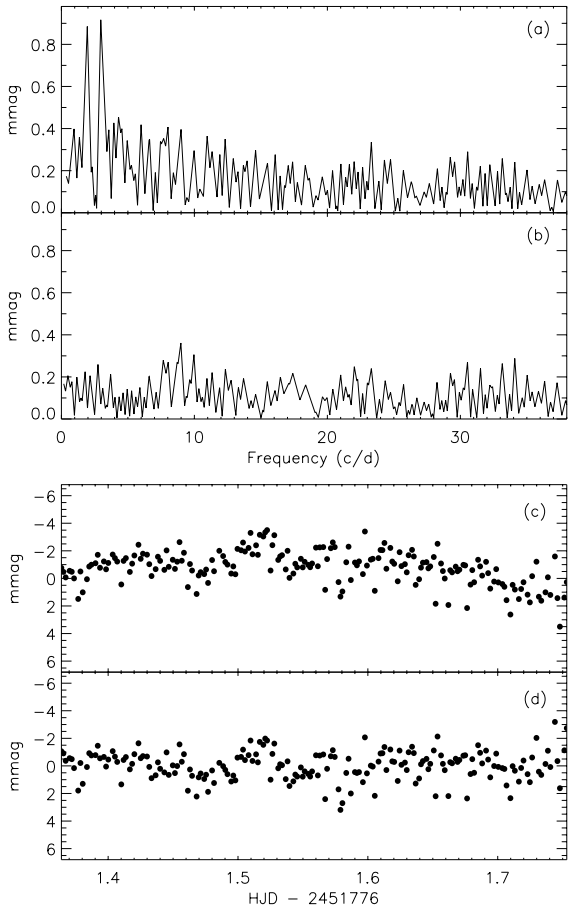

Fig. 2. Photometric quality and the effect of decorrelation for the constant star ID 143: **a)** amplitude spectra for the raw data from all nights; **b)** same as **a)** for the decorrelated data; **c)** the raw B time series from night 2; **d)** same as **c)** for decorrelated data

to 7.2 nm for B and used in the formula for both filters. The scintillation and shot noise were calculated for average exposure times of 50 and 25 s for B and V, respectively, using the same proportional factor for both filters. These estimates show that the photometric noise present in our light curves is, for a star of a given magnitude, comparable to the theoretical value, indicating that no significant systematic sources of error have been introduced in the applied observing and reduction methods. We used the formulae from Montgomery & O'Donoghue (1999) to estimate the random uncorrelated noise on a least–squares fit of the light curves. The estimated rms error on the amplitudes is given in Col. 13 of Tables 2–3. The theoretical error on the frequencies is 0.01–0.02 c d^{-1}, which we find to be 3–4 times smaller than the actual uncertainty, apart from aliasing. But as noted by Montgomery & O'Donoghue (1999) and as found for observations of XX Pyx by Arentoft & Sterken (2000), these values are only lower bounds on the actual noise. An example of the photometric quality is given in Figs. 2b and 2d for the constant star ID 143, which is one of the brightest stars ($V = 12\overset{\mathrm{m}}{.}9$) in the photometry. The noise level in the amplitude spectrum (Fig. 2b) is 0.1 mmag, and the internal rms error of the light curve (Fig. 2d) from the second night is 1.1 mmag or similar to the shot noise.

3.2. Colour–magnitude diagram

Figure 3 shows the colour–magnitude diagram for the cluster. Each magnitude was determined as the median of all points in the B and V light curves from the second night. To check for any long-period variables, this diagram was compared to one made from two successive B and V images. The dominating source of errors is the photometric transformation with 30–40 mmag rms errors in V and $B-V$, while the photometric errors are of the order of a few mmag. A large number of red stars clustering around $(B-V,\ V) = (1.8,\ 17.0)$ shows presence of several field stars. From isochrone fitting to isochrones from Bertelli et al. (1994) we find $E(B-V) = 0.42 \pm 0.05$, a distance of 2000 ± 400 pc or a distance module $m-M(V) = 12.76 \pm 0.4$ and a cluster age of 500 Myr. The dashed lines in the figure are the borders of the δ Scuti instability strip (Breger 2000). Detected and probable variables (see below) are labeled according to Tables 2–3.

3.3. Time series analysis

Light curves and amplitude spectra of all stars were searched for periodicities by visual inspection. In the following, we define "amplitude" as half of the peak–to–peak ranges. Criterion for significant detection of variability was, following Breger et al. (1993), $S/N = 4$: an amplitude of 4 times the average noise inside a box centered on the tested frequency in a prewhitened spectrum. Interesting stars were checked for effects due to CCD-position (close to image edge, nearby saturated neighbours and CCD blemishes) and rejected if questionable. The result of the manual inspection was an ensemble of 30 stars judged as being worth further examination.

3.3.1. Procedure for analysis of variability

Amplitude spectra were calculated using the Period98 v.1.0.4 (Sperl 1998) code which uses a least–squares fit of sine and cosine functions to the light curve. Figure 4 shows window functions for the B and V data. The periodograms were searched for significant frequencies between 0–40 c d^{-1}, but because of the adjustment of nightly zero–points for the B–light curves, we rejected frequencies below 5 c d^{-1}. In some cases, such as for $V3$, $V9$ and $V11$ (see below), periodicities remained significant inside this excluded range after decorrelation, typically with a frequency of 2 c d^{-1}. Such long–period variations may be instrumental or due to stellar pulsations, but since they were not removed from the data, some minor disagreements between model and observations are seen in a few cases. The only case where frequencies below 5 c d^{-1} were trusted was the star $V2$, where a clear low–frequency

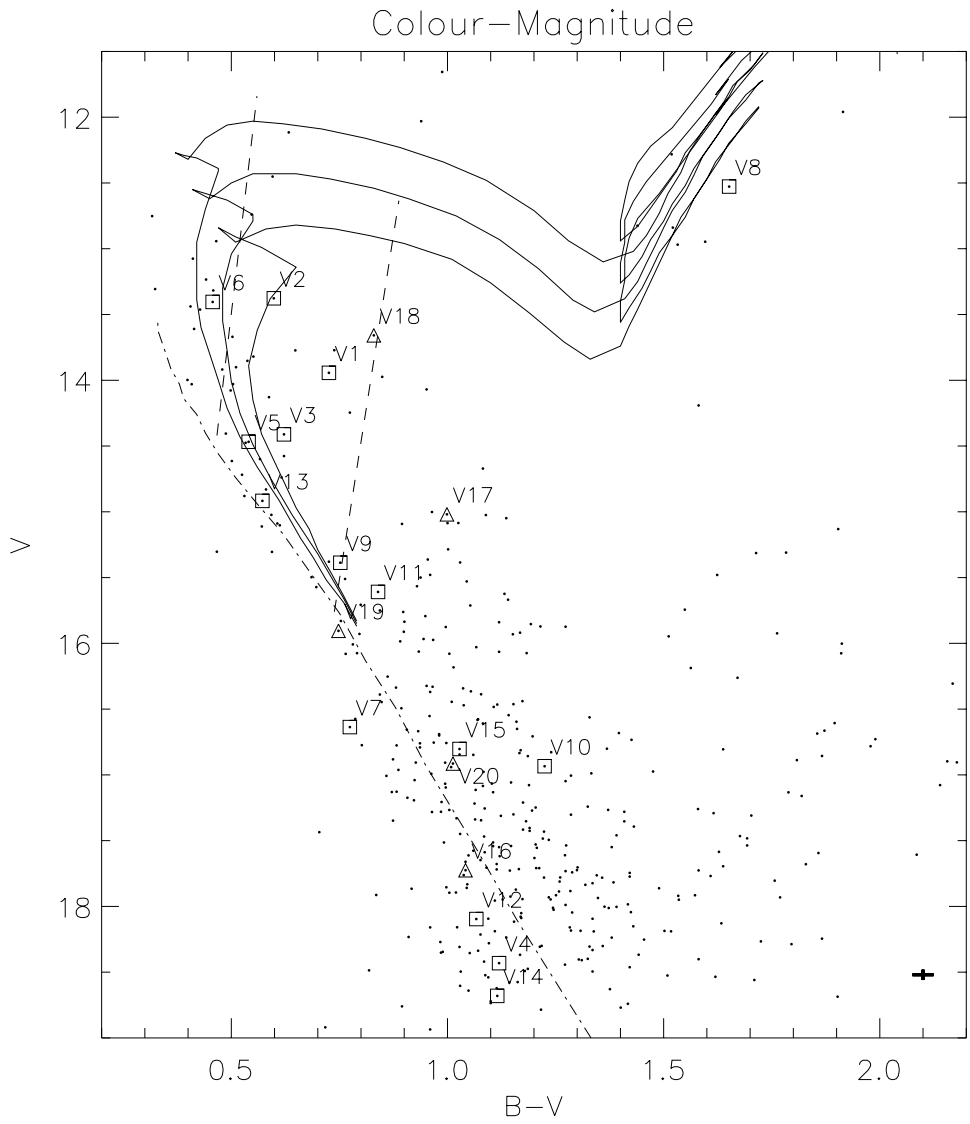

Fig. 3. Colour–magnitude diagram for our sample of 422 stars in NGC 7062. Isochrones (Bertelli et al. 1994) are plotted with full lines for log(age) = 8.6, 8.7 and 8.8, calculated for solar metal content. The ZAMS is marked with dot–dashed lines, and the δ Scuti instability strip (Breger 2000) is indicated with dashed lines. □–symbols indicate the variables $V1-V15$ and △–symbols indicate the probable variables $V16-V20$. The cross is the error bar for the photometric transformation

pulsation is present in the light curve. Here the unadjusted V light curve was used in the analysis down to 0 c d^{-1}.

Several of the 30 interesting stars showed more than one single frequency in their periodogram and for these we used the following procedure in the Fourier analysis: using a simultaneous fit with all frequencies to the original time string, we successively prewhitened the spectrum for convincing periodicities (found by identifying outstanding peaks in a spectrum prewhitened for the previous highest peaks). This was done until only noise remained, then we determined the S/N for all frequencies, based on the noise level in the residual amplitude spectrum. Insignificant frequencies were omitted from the solution, and the noise level was re–calculated in the residual spectrum prewhitened with the remaining frequencies. We iterated this procedure until only reliable detections were left. Time strings with data from all four nights were used as the default – only in the case of strong disagreement between the calculated and observed light curves for the last two nights did we limit the time series to the first two nights. In such cases the two– and four night solutions were compared and found to agree on the significant frequencies, but with a higher S/N–ratio in the two–night solution. Of the 30 stars originally selected as potential variables, 15 turned out to display variability on a statistically significant level. All detected variables, as well as 5 probable candidates, are tabulated in Tables 2 and 3. Their positions in the observed field and in the colour–magnitude diagram are shown in Figs. 1 and 3, respectively, and they are discussed individually below.

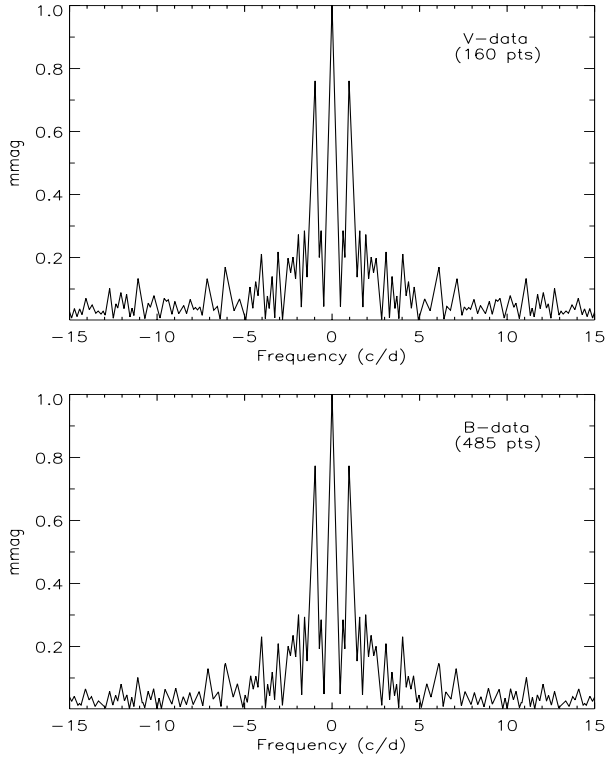

Fig. 4. Window functions for all four nights. Top: V–data. Bottom: B–data

4. Presentation of results: The variables

Tables 2 and 3 give the results of detected and probable variables in the cluster. Equatorial coordinates are based on the Hubble Space Telescope Guide Star Survey. Figures 5–14 give raw amplitude spectra and light curves from the first two nights for variables with two or more frequencies. In a single case ($V1$, see below), all prewhitened spectra are also given for the solution. In the figures, detected frequencies are marked with small vertical bars in the periodograms, and light curve models from the solutions in Table 2 are superimposed on the observed light curves. Phases for the identified frequencies are not given because of the low precision of the frequencies, but phase-lag between B and V light curves are clearly present for some of the stars. The last column in the table ("Notes", Col. 14), gives the following three properties of the stars, if known from the literature or as given by us: δ Scuti star (DS); Cluster Member (CM); and positioned in the δ Scuti star Instability Strip (IS).

We take a star to be a δ Scuti star if it has one or more significant (4σ) frequencies in the range 4–50 c d^{-1}, down to 1 c d^{-1} for evolved stars, and amplitudes below $V = 0\overset{\mathrm{m}}{.}5$ (Breger 2000). Additional criteria are if the variable has a rich periodogram or if beating between close frequencies is seen in the light curve. Cluster membership is designated when known from Peniche et al. (1990), or when the star is located on the cluster isochrone in the colour–magnitude diagram, within the errors. A δ Scuti star must be in the instability strip in order to be a cluster member, thus stars in Table 2 classified as "DS" only, are field δ Scuti stars.

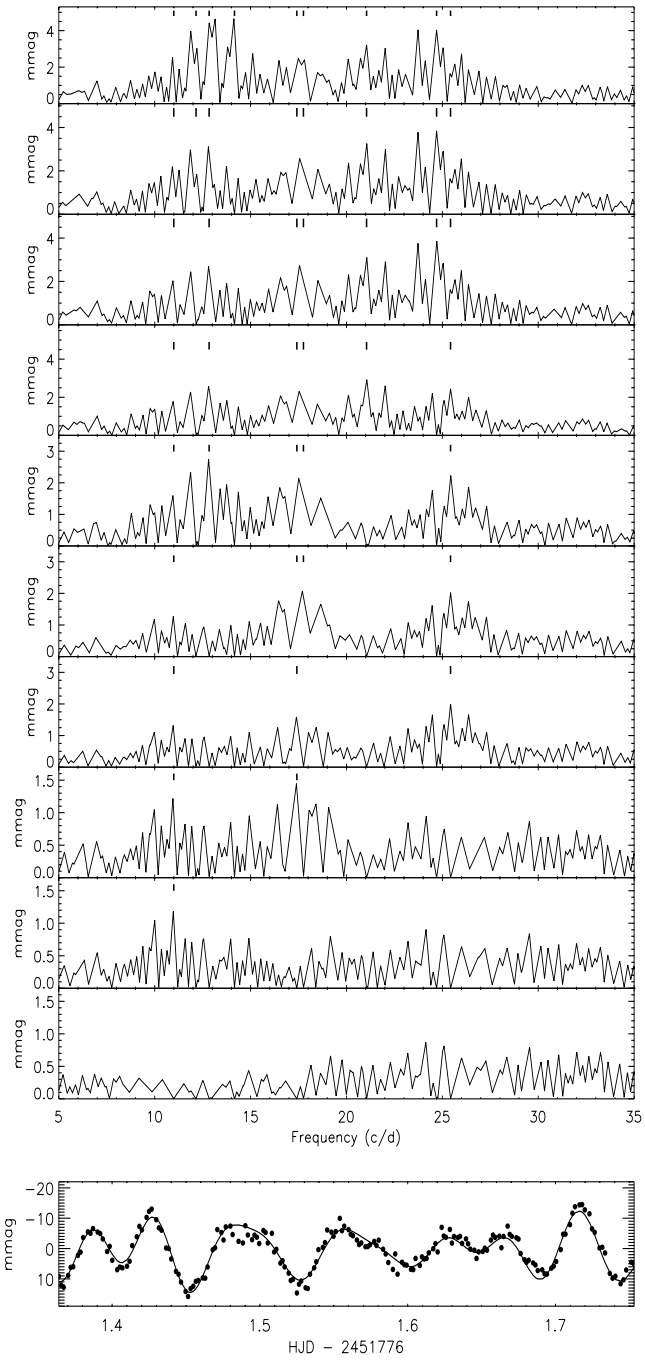

Fig. 5. Amplitude spectra of star $V1$. From top to bottom is given the raw and successively prewhitened amplitude spectra. The lower panel is the B light curve from the second night. Detected frequencies are marked in the individual spectra

Below, we discuss the individual δ Scuti stars and −candidates. The first, $V1$, is the same star as #180 from Viskum et al. (1997). The two candidate variables from Peniche et al. (1990) (see above) were also checked for variability: ID 13 ($V = 13\overset{\mathrm{m}}{.}1$) is positioned just outside the blue edge of the instability strip, but the light curves are constant down to the noise level of 2 mmag; ID 17

Table 2. Basic and pulsational data for the detected variable stars $V1$–$V15$ in NGC 7062. *Columns 1–3*: cross–identifications to star numbers from Hoag et al. (photographic data, 1961) and Peniche et al. (1990). *Column 9*: S/N ratio in B band (V for $V2$). *Columns 10–11*: semi–amplitudes a_B and a_V in B and V. *Column 12*: theoretical photon shot noise, $\sigma(m_B)$, for the B data. *Column 13*: typical 1σ amplitude errors from random noise in the least–squares fit. *Column 14*: classifications (see text) as δ Scuti star (DS), Cluster Member (CM) and location inside the Instability Strip (IS)

ID	Hoag	Pen.	$\alpha_{2000.0}$ [hh:mm:ss]	$\delta_{2000.0}$ [$^\circ:':''$]	V	$B-V$	f c d^{-1}	S/N	a_B mmag	a_V* mmag	$\sigma(m_B)$ mmag	$\sigma(a_B)$ mmag	Notes
$V1$	50	44	21:23:29.81	46:22:38.6	13.94	0.73	14.2	16.7	2.7	2.3	1.9	0.1	DS, CM, IS
							12.2	12.6	1.9	1.6			
							24.7	9.5	3.8				
							21.0	8.3	2.9				
							12.8	19.7	3.1	2.3			
							17.8	7.5	2.0				
							25.4	5.1	2.0				
							17.4	6.2	1.6				
							11.0	11.3	1.8				
$V2$	35	16	21:23:30.62	46:21:38.4	13.38	0.60	4.6	21.7	11.7	10.4	1.5	0.2**	DS, CM, IS
							2.6	6.1	5.2	4.7			
							7.4	5.5	3.2	2.8			
$V3$	60	29	21:23:35.86	46:24:11.1	14.41	0.62	19.2	9.6	4.7	3.6	2.3	0.1	DS, CM, IS
							13.5	9.9	4.2	2.8			
							19.5	4.6	2.2				
							11.5	4.6	1.7				
$V4$			21:23:29.76	46:23: 5.0	18.43	1.12	21.6	8.8	29.2	14.0	18.3	1.2	DS
							5.7	6.0	19.7				
							22.5	6.0	19.7				
							20.9	4.4	14.6				
$V5$		32	21:23:21.72	46:25:12.4	14.47	0.54	20.2	7.6	3.2	1.8	2.3	0.1	DS, CM, IS
							21.0	7.1	3.0				
							22.4	6.4	2.7				
$V6$	46		21:23:21.58	46:22:60.0	13.41	0.46	13.3	7.0	2.0	1.	1.3	0.1	DS, CM, IS
							11.1	4.7	1.2	1.			
$V7$			21:23:46.34	46:26: 0.6	16.64	0.77	30.2	6.2	6.8	5.0	6.8	0.4	DS
							22.4	4.8	4.9				
							28.0	5.5	4.7	6.0			
$V8$	21	58	21:23:13.68	46:20:51.8	12.53	1.65	6.6	6.0	2.0	1.7	1.5	0.1	CM
							9.6	4.9	1.4				
							13.5	4.7	1.2				
$V9$	94	55	21:23:40.18	46:23:56.3	15.39	0.75	18.1	21.1	5.7	4.6	3.8	0.2	DS, IS, CM
$V10$			21:23:22.97	46:22:25.4	16.93	1.23	12.1	9.3	7.5	3.8	9.6	0.6	DS
							17.3	4.5	4.0				
$V11$			21:23:33.50	46:22: 8.0	15.61	0.84	11.6	7.1	2.4	1.6	4.4	0.3	DS, CM, IS
							11.1	6.5	2.1				
$V12$			21:23:14.11	46:24:40.9	18.10	1.07	9.3	8.1	30.8	11.8	15.3	1.0	DS
$V13$		25	21:23:18.53	46:21:23.3	14.92	0.57	12.4	7.0	2.6	1.8	2.8	0.2	DS, CM, IS
$V14$			21:23:39.14	46:20:21.4	18.68	1.12	7.1	5.4	11.8		20.5	1.3	DS
$V15$			21:23:23.86	46:22:58.7	16.80	1.03	10.0	4.3	4.3	6.3	8.3	0.5	

* Time series are not decorrelated or corrected for nightly zero-points.
** Noise calculated for the V time series.

($V = 12\overset{\mathrm{m}}{.}8$) qualifies as a blue straggler, but also here no oscillations were detected down to 2 mmag. A single visible peak in the periodogram of ID 17, at 15.3 c d^{-1} with $S/N = 3.6$ and 0.6 mmag amplitude, is below detection.

4.1. Multimode variables

4.1.1. NGC 7062 V1

Peniche et al. (1990) found that this star belongs to the cluster and Viskum et al. (1997) discovered that it was a potential δ Scuti star with 10 mmag amplitude and is placed in the middle of the instability strip. The light

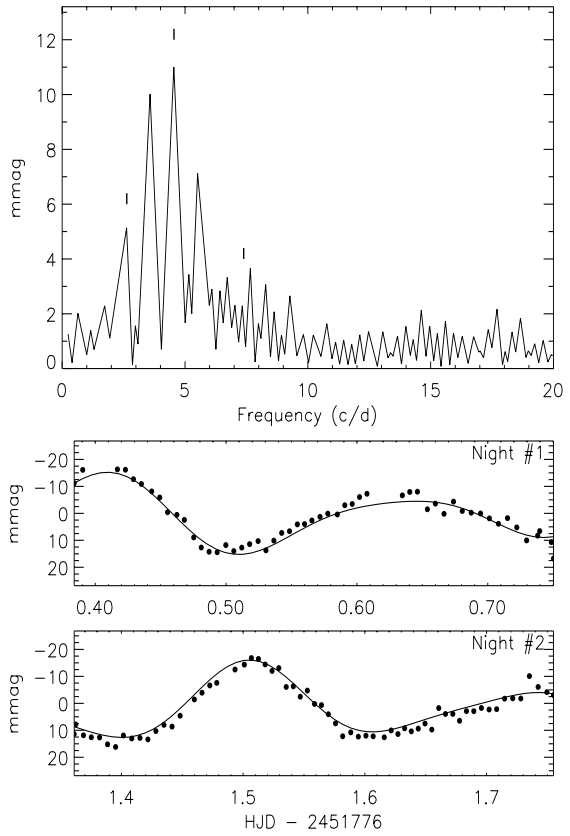

Fig. 6. Amplitude spectrum of star $V2$ and V light curves for the two first nights. Note the two 30 min gaps in the light curve from the first night, which are due to scheduled service observations in the beginning and in the last half of the night

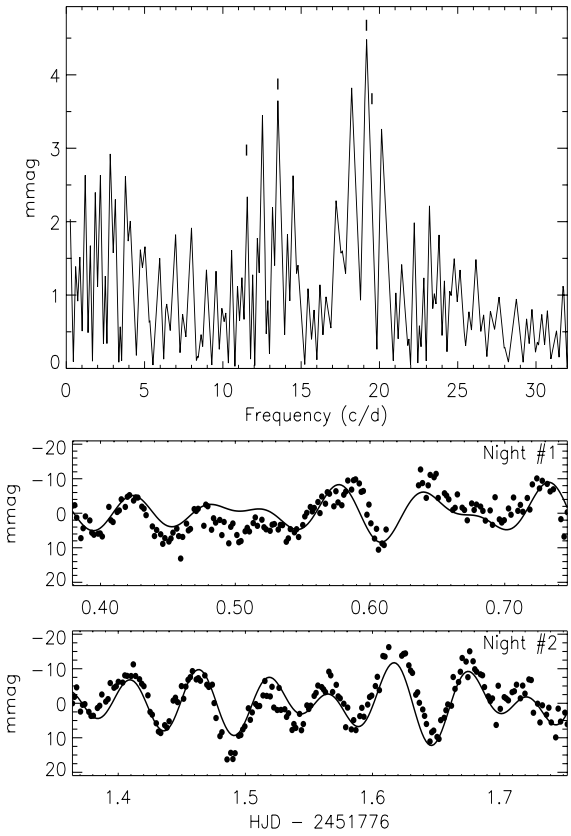

Fig. 7. Amplitude spectrum and B light curves of star $V3$. Note the overall agreement between the four–frequency solution and the data, though some additional frequencies might remain undetected

curve by Viskum et al. (1997, their Fig. 10) suggests a frequency of $\sim$11 c d^{-1}. We confirm the position inside the instability strip, slightly towards the red edge and as seen in Fig. 5, this star is clearly a multi–periodic δ Scuti star. In the periodogram we detect 9 frequencies and more are probably present since the solution, superimposed on the figure, is insufficient to fit all details of the observations.

4.1.2. NGC 7062 V2

This is a member of the cluster, positioned on the blue edge of the instability strip just after the turn-off point. The star is clearly variable, having a high amplitude with variations. The periodogram for the B–photometry shows a significant frequency below 5 c d^{-1}, but in order to avoid the aforementioned effects of nightly zero–point corrections on low–frequency modes, we used the non–decorrelated V–photometry which was not corrected for nightly magnitude shifts. The V data confirm the periodicity (Fig. 6) and we find three significant frequencies: 4.5, 2.6 and 7.4 c d^{-1}. The position of $V2$ in the colour–magnitude diagram on the blue side of the red edge rejects the possibility of it being a γ Doradus star. Instead we believe it to be a massive ($M > 2\ M_{\odot}$) δ Scuti star with longer periods due to its evolutionary stage (Breger 2000).

4.1.3. NGC 7062 V3

This star is a cluster member and is positioned right in the center of the instability strip. The light curve (Fig. 7) shows clear multi–periodic, short-period oscillations. In the periodogram we detect 4 frequencies: 19.2, 13.5, 19.5 and 11.5 c d^{-1} having amplitudes of 2–5 mmag. This solution fits the light curve well, except for some details which suggest that the solution is not complete. $V3$ is a δ Scuti star.

4.1.4. NGC 7062 V4

Positioned on the ZAMS, far from the cluster turn–off and instability strip, this star is one of the faintest variables in the sample. The light curve and amplitude spectrum are presented in Fig. 8. The light curve is noisy, but shows evidence of multi–periodicity/beating, which is supported by the amplitude spectrum. Using light curves from the first two nights only, we detect 4 frequencies, 3 of which are in a very narrow frequency band. They seem to describe the light curve well. Frequencies and amplitudes suggest δ Scuti type variability, but based on the position in the colour–magnitude diagram, the star is probably not a physical member of the cluster. No information on membership for this star is available.

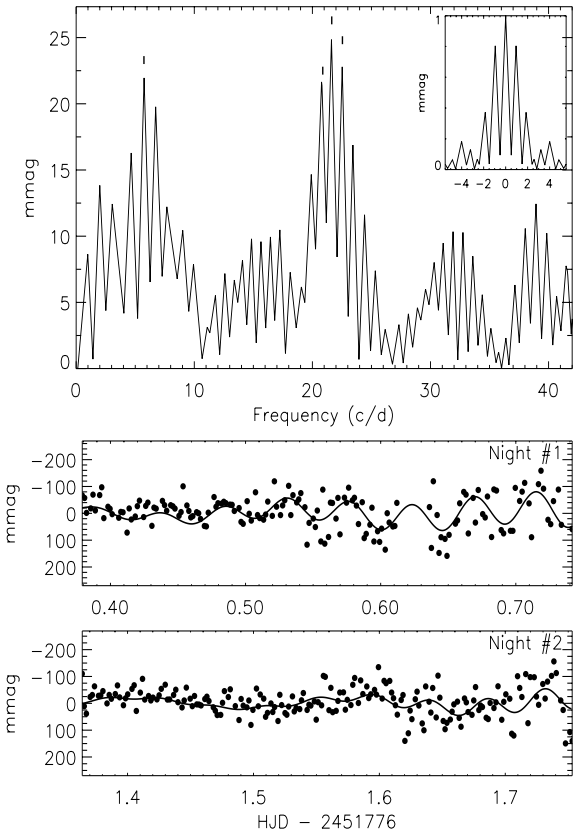

Fig. 8. Amplitude spectrum and B light curves of star $V4$. Only the first two nights were used for the fitting and the corresponding window function has been inserted

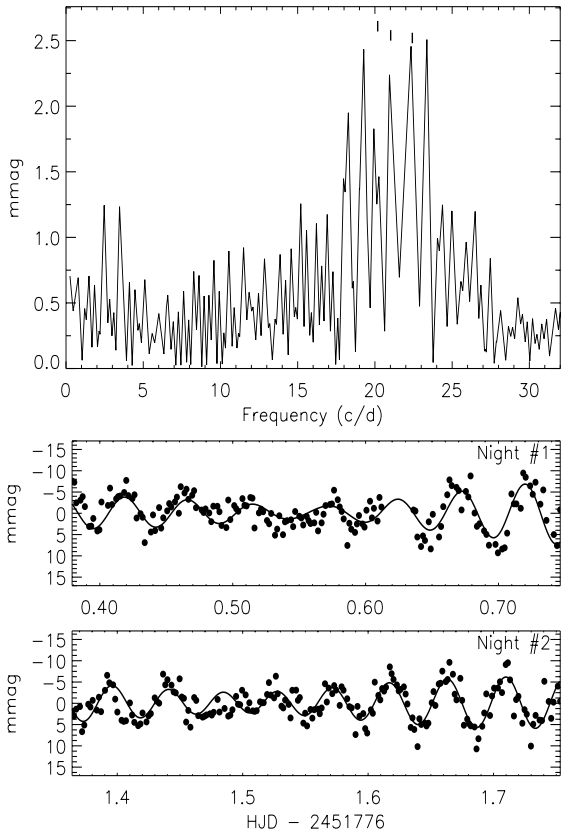

Fig. 9. Amplitude spectrum and B light curves of star $V5$

4.1.5. NGC 7062 V5

The light curve of this star (Fig. 9) shows that it is a clear short–period variable, with beating between several modes. The star is located inside the instability strip, near the blue edge, coinciding with the $\log(\text{age}) = 8.8$ isochrone and is a cluster member. Beating is evident in the light curve and the multi–periodicity is confirmed by the amplitude spectra. We detect 3 closely–spaced frequencies around 20 c d^{-1}, which altogether represent a reasonable fit to the light curve. The amplitudes are around 3 mmag for all frequencies and the star is clearly a δ Scuti star.

4.1.6. NGC 7062 V7

This star is clearly variable, having an amplitude of 20 mmag at high frequency. In the colour–magnitude diagram it is positioned about 1 mag below the instability strip at a pre–main sequence location, so we assume that it is not a cluster member. The light curve (Fig. 10) shows beating, thus multiple modes are present. We detect 3 frequencies, f_1, f_2 and f_3: 30.2, 22.4 and 28.0 c d^{-1}. The ratio $f_2/f_3 = 0.80$ agrees with theoretical values for the first two overtones of radial modes. All this suggests that $V7$ is a δ Scuti star. Just below the detection limit, a fourth frequency $f_4 = 26.2$ c d^{-1} is seen in the periodogram and

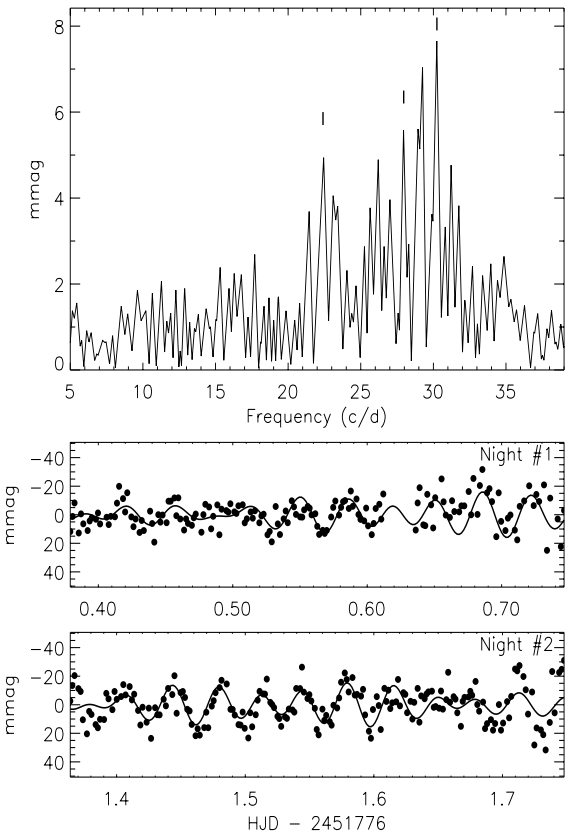

Fig. 10. Amplitude spectrum and B light curves of star $V7$

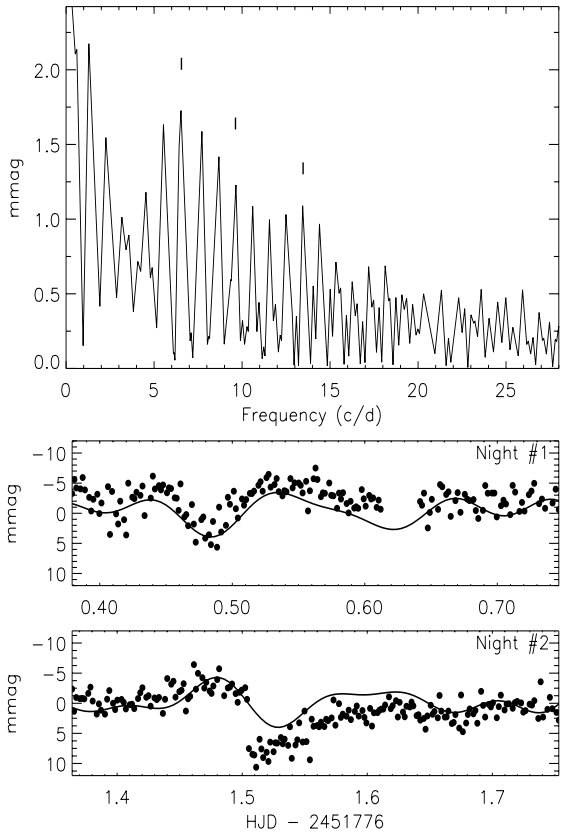

Fig. 11. Amplitude spectrum and B light curves of star $V8$

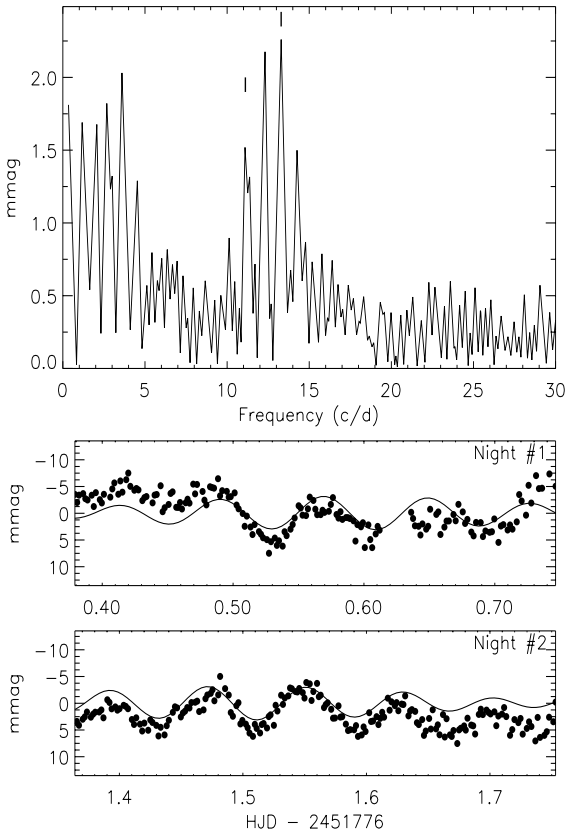

Fig. 12. Amplitude spectrum and B light curves of star $V6$

improves the goodness of the least–squares fit considerably if included in the solution. f_4 was rejected and the theoretical model in Fig. 10 was computed using the three frequencies only, while the S/N–ratios in Table 2 were determined in a spectrum prewhitened with f_1, f_2, f_3 and f_4.

4.1.7. NGC 7062 V8

This is the brightest star among these variables: $V = 12\overset{\text{m}}{.}6$. It is located at a highly evolved position in the colour–magnitude diagram, at the red giant or core helium burning phase. No membership information is available for this star, but its location on the cluster isochrone in Fig. 3 suggests that it belongs to the cluster. The light curve resembles that of an eclipsing binary, but its shape could also be due to beating between two modes. Three frequencies are detected: 6.6, 9.6 and 13.5 $\mathrm{c\,d^{-1}}$ and reproduce the observations reasonably. The light curve from the second night (Fig. 11) shows an abrupt drop in brightness followed by a slow brightening. Such a light curve is not characteristic for either eclipsing binaries or pulsating variables. Additional observations are clearly needed to determine the nature of this star.

4.2. Single– and double mode variables

4.2.1. NGC 7062 V6

This star is located close to the instability strip, just outside the blue edge, at the cluster turn–off point. The light curves and amplitude spectrum (Fig. 12) all show signs of low–amplitude multi–periodicity (beating). The amplitude spectrum is affected by strong $1/f$–noise at low frequencies, which is only partly removed by decorrelation (mainly with air mass). Two frequencies $f_1 = 13.3$, $f_2 = 11.1$ (Table 2) are detected, but do not describe the light curve completely – mainly due to underlying low frequencies from the $1/f$–noise. Data from the last two nights are noisy, but if they are omitted, f_1 moves to its 1 $\mathrm{c\,d^{-1}}$ alias at 12.3 $\mathrm{c\,d^{-1}}$ leaving f_2 below detection. With all data, f_1 and f_2 are both detected and the model light curve reproduces the amplitude variations of the observations. The V data confirm both frequencies. As discussed for $V2$, evolved massive stars should have relatively long periods. $V6$ is located close to $V2$ in the colour–magnitude diagram, but is less evolved, which might explain its shorter periods.

4.2.2. NGC 7062 V9

The light curve indicates high correlation with air mass, but this is to some extent removed by decorrelation. Beating is seen in the light curve which suggests that two close modes are excited, but in the periodogram only a

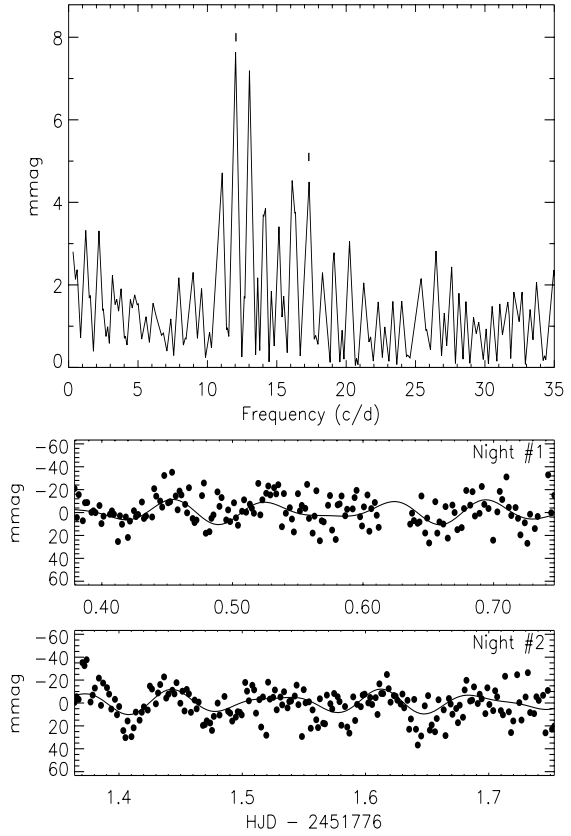

Fig. 13. Amplitude spectrum and B light curves of star $V10$

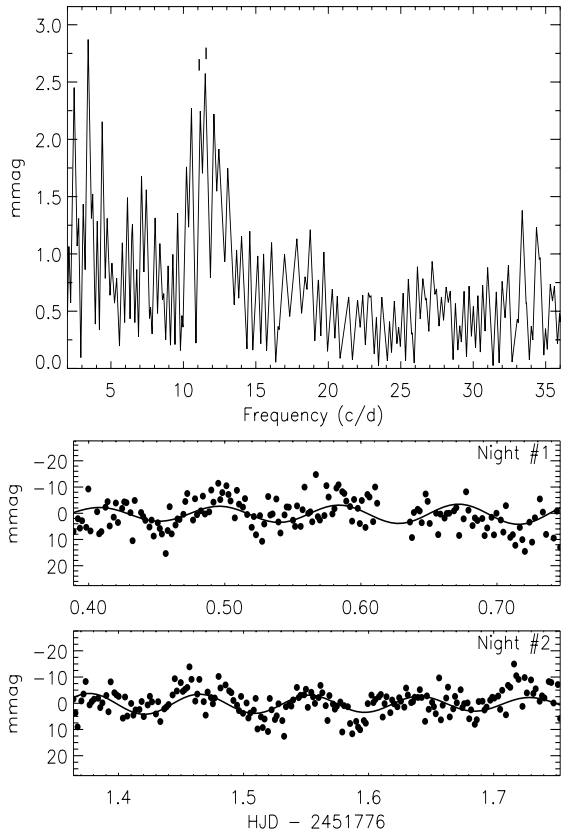

Fig. 14. Amplitude spectrum and B light curves of star $V11$

single frequency is detected at $\sim$18 c d^{-1}. The model light curve is insufficient to reproduce the amplitude variations in the observed light curve. Positioned exactly on the red edge of the instability strip, $V9$ is an interesting star for testing models predicting the red edge's position in the colour–magnitude diagram, such as from Houdek (2000). Light curves and period indicate that $V9$ is a δ Scuti star.

4.2.3. NGC 7062 V10

This is a faint star positioned slightly off the main–sequence and cluster membership is not known. The star exhibits a short–period variability with amplitude variations (Fig. 13). Two frequencies are detected: 12.1 and 17.3 c d^{-1}. If $V10$ indeed is not a cluster member, at least one of the frequencies are non–radial as compared to theoretical period ratios from Breger (2000).

4.2.4. NGC 7062 V11

This star is positioned close to the main sequence near the red edge of the instability strip. It is clearly variable having a low amplitude, and in the periodogram we find two close frequencies at 11.6 and 11.1 c d^{-1} which cause a visible beating in the light curve. A frequency below 5 c d^{-1} (Fig. 14) is only present in the B time series. The position on the main–sequence suggests that $V11$ is a cluster member. $V11$ has a $0\overset{\mathrm{m}}{.}5$ fainter, close neighbour with a constant time series.

4.2.5. NGC 7062 V12

Positioned close to the ZAMS among the faintest stars detected in the field, the light curve of this star is very noisy. A nearly sinusoidal variation is clearly present in the light curve, and the amplitude spectrum reveals an oscillation frequency of fairly high amplitude (30 mmag) – seemingly the only one present in the light curve. No other periods are found in the prewhitened data. The noise–level is rather high (3.8 mmag in the amplitude spectrum after prewhitening), but the frequency is clearly significant.

4.2.6. NGC 7062 V13

This star is a main–sequence star placed in the center of the instability strip, and was found to be a member star by Peniche et al. (1990). The light curve shows a clear low–amplitude variability with beating. Only a single frequency is significant in the periodogram at 12.4 c d^{-1} but it does not agree completely with the light curve. A second frequency at 8.0 c d^{-1} seems to improve the agreement between model and data, but was rejected due to a low S/N ratio of 3.6. The star has a close neighbour (Fig. 1) which is constant and of similar magnitude, and correlation with seeing does not change the solution. $V13$ is a δ Scuti star.

Table 3. Same as Table 2 but for the probable variables $V16$–$V20$

ID	Hoag Pen.	$\alpha_{2000.0}$ [hh:mm:ss]	$\delta_{2000.0}$ [°:′:″]	V	$B-V$	f c d^{-1}	S/N	a_B mmag	a_V^* mmag	$\sigma(m_B)$ mmag	$\sigma(a_B)$ mmag	Notes
$V16$		21:23:17.74	46:22: 8.3	17.73	1.04	12.0	7.6	17.5	9.8	12.8	0.8	
						19.1	5.4	13.6	6.9			
$V17$		21:23:44.52	46:24:20.0	15.0	1.0	2.1	7.2	3.3	4.0	3.6	0.2	
						5.0	5.0	2.3				
$V18$	51	21:23:38.54	46:20:32.3	13.66	0.84	4.0	5.1	1.8		1.8	0.1	IS
$V19$		21:23:35.93	46:23:20.9	15.91	0.75	3.2	4.7	2.8	3.0	4.8	0.3	IS
$V20$		21:23:31.61	46:22:18.0	16.91	1.01	6.6	4.4	4.4	3.5	8.6	0.6	

* Time series are not decorrelated or corrected for nightly zero-points.

4.2.7. NGC 7062 V14

This ZAMS–star is again very faint, but with a light curve showing clear signs of variability. We only find a single oscillation present at a significant level, with a frequency of 7.1 c d^{-1} and an amplitude of about 12 mmag. One additional frequency at 13.2 c d^{-1} is also likely to be present, though below our detection criteria, but both frequencies together reproduce the the observed light curve well.

4.2.8. NGC 7062 V15

This star is positioned close to $V20$ in the colour–magnitude diagram, slightly off the ZAMS. No information on cluster membership is available. A single frequency is detected ($S/N = 4.3$) at 10.0 c d^{-1} and is confirmed by the V photometry. Peculiarly, the amplitude is larger in the V band, but $1/f$–noise is high and therefore the difference is probably insignificant. This star has a close neighbour which is constant and 4 mag brighter.

4.3. Probable variables

4.3.1. NGC 7062 V16

This star is very faint and red ($V = 17.8$, $B-V = 1.1$), but positioned on the ZAMS. The light curve is suspicious: two flare–like peaks with $0\overset{\mathrm{m}}{.}1$ amplitude occuring around – but not exactly at – the same time during the first two nights. The photometry may be influenced by bleeding charges from a close saturated star on the CCD, which seems confirmed by a strong correlation with the x–position. We therefore cannot exclude instrumental effects here and reject the star from the sample of detected variables. In the periodogram, we detect the frequencies 12.0 and 19.1 and the solution is reasonable, but incomplete. Better data should be obtained for this star.

4.3.2. NGC 7062 V17

It appears from the light curve shape that this star is variable and in the amplitude spectrum, two frequencies are detected. We have classified the star as a probable variable because at least one of the frequencies (2.1 c d^{-1}) is below the 5 c d^{-1} limit. The variability in the B–data is not confirmed by the V–data due to a too high noise level. We believe this to be a variable star, but the detected frequencies are not reliable in the present dataset.

4.3.3. NGC 7062 V18

This star is positioned on the red border of the instability strip (see Fig. 3) and has a frequency of 4.9 c d^{-1} just below the detection limit ($S/N = 3.7$). The light curve shows abrupt drops in brightness at about the same moment the first two nights. The amplitude of the calculated model is too low to fit the observations. The variable nature can be of eclipsing or pulsating origin. No instrumental effects seem to be the source of these variations.

4.3.4. NGC 7062 V19

This star is located on the ZAMS and just outside the red edge of the instability strip in the colour–magnitude diagram. The light curve shows a slow variation of 3 mmag amplitude. We detect the frequency 3.2 c d^{-1} in the decorrelated B–data but at 2.0 c d^{-1} in the V–data. The star seems not to be affected by other stars or from instrumental effects. Because of our criterion of frequencies above 5 c d^{-1}, $V19$ is rejected from the sample of detected variables, but should be investigated further.

4.3.5. NGC 7062 V20

This star is positioned away from the main-sequence as noticed by Peniche et al. (1990) and thus may not be a cluster member. It is furthermore placed well outside the instability strip in the colour–magnitude diagram. The star is faint and the observations are noisy but a periodic variation is seen. In the periodogram we detect the frequency 6.6 c d^{-1}, but because the star has a 4 mag brighter neighbour and furthermore is close to a CCD blemish, we reject it from our sample of detected variables but encourage further observations.

5. Conclusions

We have presented fifteen variables ($V1$–$V15$) found in the field of NGC 7062, of which one was known hitherto ($V1$). Ten of these ($V1$–$V8$, $V10$–$V11$) are oscillating in two or more frequencies simultaneously, and eight stars ($V1$–$V3$, $V5$, $V6$, $V9$, $V11$, $V13$) are inside or near the δ Scuti instability strip. A number of these stars have beautiful light curves where up to 9 frequencies are detected, which together with the cluster's suitability for observing with typical telescopes makes the cluster an excellent target for a multisite campaign.

The number of known variable stars in the cluster has been increased considerably. We have shown that ∼20% of stars inside the cluster IS show signs of variability above the 0.7–4.5 mmag level for the corresponding magnitude range $B = 12\overset{\mathrm{m}}{.}5-16\overset{\mathrm{m}}{.}5$.

Of the fifteen variables, we deem thirteen to be δ Scuti stars – eight belonging to the cluster ($V1$–$V3$, $V5$, $V6$, $V9$, $V11$, $V13$) and other five ($V4$, $V7$, $V10$, $V12$, $V14$) which probably are field stars, as determined from their position in the colour–magnitude diagram.

The variables $V8$ and $V15$ require longer observing runs and new Strömgren photometry in order to determine the nature of their variability and if they are members of NGC 7062. The presented photometry was optimised for 12^{m} stars, so future investigations of the more faint variables in the presented sample would need to be optimised for $\sim 14^{\mathrm{m}}$ – an effort to be considered in proportion to their value as probable non–members of the cluster.

In addition to the 15 variables, we found 5 probable variables ($V16$–$V20$), for which further observations are needed for verification/determination of their variability. No High–Amplitude δ Scuti stars were found.

Acknowledgements. Part of this research was carried out in the framework of the project IUAP P4/05 financed by the Belgian DWTC/SSTC. This work has been supported by the Belgian Fund for Scientific Research (FWO) and has made use of the Simbad database, operated by the CDS, Strasbourg, France. Data reduction and -analysis made use of the `MOMF` and the `NOAO-IRAF` software. We thank E. Michel for a careful reading of the paper. The data presented here have been taken using ALFOSC, which is owned by the Instituto de Astrofisíca de Andalucia (IAA) and operated at the Nordic Optical Telescope under agreement between IAA and the NBIfAFG of the Astronomical Observatory of Copenhagen.

References

Arentoft, T., & Sterken, C. 2000, J. Astron. Data, 6, 4C
Arentoft, T., Kjeldsen, H., Bedding, T. R., et al. 1998, A&A, 338, 909
Belmonte, J. A., Michel, E., Alvarez, M., et al. 1994, A&A, 283, 121
Bertelli, G., Bressan, A., Chiosi, C., et al. 1994, A&AS, 106, 275
Breger, M. 2000, in Proceedings of the Delta Scuti and Related Stars, Vienna 4–7 August, 1999, Astron. Soc. Pac. Conf. Ser., 210, 3
Breger, M., Stich, J., Garrido, R., et al. 1993, A&A, 271, 482
Breger, M., Zima, W., Handler, G., et al. 1998, A&A, 331, 271
Breger, M., Handler, G., Garrido, R., et al. 1999, A&A, 349, 225
Frandsen, S., & Arentoft, T. 1998a: "STACC open cluster target list", J. Astron. Data, 4, 6
Frandsen, S., & Arentoft, T. 1998b, A&A, 333, 524
Frandsen, S., & Kjeldsen, H. 1993, in Proceedings of Inside the Stars, IAU Coll. 137, Astron. Soc. Pac. Conf. Ser., 40, 47
Frandsen, S., Pigulski, A., et al. 2000, in The Impact of Large-Scale Surveys on Pulsating Star Research, IAU Coll. 176, Astron. Soc. Pac. Conf. Ser., 203, 473
Frandsen, S., Balona, L. A., Viskum, M., Koen, C., & Kjeldsen, H. 1996, A&A, 308, 132
Handler, G., Arentoft, T., Shobbrook, R. R., et al. 2000, MNRAS, 318, 511
Hassan, S. M. 1973, A&AS, 9, 261
Hoag, A. A., Johnson, H. L., Iriarte, B., et al. 1961, in Publications of the United States Naval Observatory, Second Series, vol. 17, part 7
Houdek, G. 2000, in Proceedings of the Delta Scuti and Related Stars, Vienna 4–7 August, 1999, Astron. Soc. Pac. Conf. Ser., 210, 454
Kjeldsen, H., & Frandsen, S. 1992, PASP, 104, 413
Montgomery, M. H., & O'Donoghue, D. 1999, Delta Scuti Star Newsletter, 13, 28, University of Vienna
Peniche, R., Peña, J. H., Diaz-Martinez, S. H., & Gomez, T. 1990, Rev. Mex. Astron. Astrofis., 20, 127
Sperl, M. 1998, User manual Period98, Institute of Astronomy, University of Vienna
Viskum, M., Hernández, M. M., Belmonte, J. A., & Frandsen, S. 1997, A&A, 328, 158
Winget, D. W. 1993, GONG 1992, in Proceedings of Seismic Investigation of the Sun and Stars, Boulder, Colorado August 11–14, 1992, Astron. Soc. Pac. Conf. Ser., 42, 331